Asymptotic description of wave propagation in an active Lorentzian medium

Reza Safian, Mohammad Mojahedi, and Costas D. Sarris
The Edward S. Rogers Sr. Department of Electrical and Computer Engineering, University of Toronto, Toronto, Ontario, Canada M5S 3G4

(Received 20 November 2006; revised manuscript received 22 February 2007; published 26 June 2007)

In a causally dispersive medium the signal arrival appears in the dynamical field evolution as an increase in the field amplitude from that of the precursor fields to that of the steady-state signal. The interrelated effects of phase dispersion and frequency dependent attenuation and/or amplification alter the pulse in such a fundamental way that results in the appearance of precursor fields. Although superluminal group velocities have been found in various dispersive media, the pulse "front" and associated precursors will never travel faster than c, and hence these are the vehicles through which relativistic causality is preserved. While many rigorous studies of wave propagation and associated abnormal group velocities in passive Lorentzian media have been performed, the corresponding problem in active media has remained theoretically unexplored. This problem is addressed in the present paper, by employing the steepest descent method for the determination of the response of an active Lorentzian medium to a step modulated pulse. The steepest descent method provides a detailed description of the propagation of the pulse inside the dispersive medium in the time domain. Moreover, the evolution of the saddle points illuminates the relation between the medium parameters and the temporal evolution of the propagating pulse within the medium. Hence, useful physical insights are obtained and the interesting differences between the passive and active case are deduced.

DOI: 10.1103/PhysRevE.75.066611 PACS number(s): 42.25.Fx, 02.70.Bf, 73.40.Gk

I. INTRODUCTION

Wave propagation through a linear, temporally dispersive medium has been a complex and sometimes controversial research topic since the 19th century. In a dispersive medium, each spectral component of the initial pulse propagates with its own phase velocity and absorption-amplification rate. Hence, the phase relation and the relative amplitudes between the spectral components of the initial pulse change as a pulse propagates inside the medium. Superluminal group velocities which are the direct consequence of medium dispersion, have been theoretically predicted and experimentally observed in various types of dispersive media, such as Lorentzian media, one-dimensional photonic crystals, and undersized waveguides [1–19]. Though superluminal group velocities have been found in these media, it has been suggested that the pulse "front" and associated transient field oscillations, known as the precursors or forerunners, will never travel faster than c, and hence relativistic causality is always preserved [4].

Sommerfeld and Brillouin were among the early researchers studying the wave propagation in linear, homogeneous, isotropic, causally dispersive media [20]. They used the asymptotic method of steepest descent to describe the propagation of a modulated unit step signal of constant carrier frequency (ω_c) in a semi-infinite single resonance passive Lorentz medium. Their analysis led to the discovery of two wave phenomena whose dynamical evolution preceded the evolution of the main signal. They referred to these as forerunners or precursors. The first precursor (Sommerfeld's precursor) determines the earliest time behavior of the wave which also contains the highest frequency components of the signal and the second precursor (Brillouin precursor) contains the low frequency components. In addition to Brillouin and Sommerfeld, other researchers, especially Oughstun and co-workers have done an extensive work on the same topic by refining and generalizing Sommerfeld and Brillouin work [21–32].

The possibility of superluminal propagation in an inverted two-level atomic medium was considered by Chiao [10]. He also mentions that the resulting superluminal propagation is not a violation of relativistic causality, since the information contained in the peak of the pulse is already included in the forward tail. Recently, there has been experimental observation of superluminal velocities in active media [12,14]. In light of these theoretical and experimental observations the study of the precursor fields in such media deserves closer attention. This problem is addressed in the present paper, using the steepest descent method.

Asymptotic methods such as the steepest descent provide a rigorous general solution to the problem of propagation in causally dispersive media for pulses of arbitrary duration. The method requires that the behavior of the complex phase function appearing in the integral representation of the propagated field be known throughout the complex frequency plane. Therefore a specific model of the complex refractive index is needed. The single-resonance Lorentz model which is of general interest in optics, is used in this paper.

This paper is organized as follows. In Sec. II, we present the active Lorentzian medium, which is a model for an inverted two level atomic medium. In Sec. III, the superluminal propagation of a Gaussian pulse is calculated using the inverse Fourier transform method. In Sec. IV, the general formulation of the problem of wave propagation inside a dispersive medium is provided. Section V includes the asymptotic analysis of the wave propagation in an active Lorentzian medium using the asymptotic technique of steepest descent method.

 ©2007 The American Physical Society

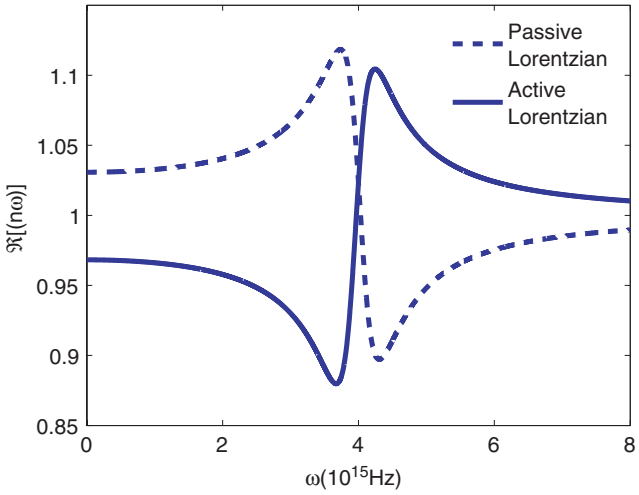

FIG. 1. (Color online) The real part of the refractive index for the two-level atomic medium in inverted state (solid line) and ground state (dashed line).

II. LORENTZIAN MEDIUM WITH INVERTED ATOMIC POPULATION

It is well known that the inversion of level populations in an atomic material leads to gain for light tuned to the resonance frequency of the two levels. The simplest example is a Lorentzian dielectric with negative oscillator strength. Ignoring the effect of inhomogeneous line broadening, the complex index of refraction for the active Lorentzian is [10]

$$n(\omega) = \left(1 + \frac{\omega_p^2}{\omega^2 - \omega_0^2 + 2\delta i\omega}\right)^{1/2}, \tag{1}$$

where, ω_0 is the frequency difference between the two levels (resonance frequency), ω_p is the plasma frequency, and δ is the linewidth of the resonance. In this model the square of the atomic plasma frequency is defined as

$$\omega_p^2 = \frac{4\pi N|f|e^2}{m}, \tag{2}$$

where f, N, e, and m are the oscillator strength, atomic density, electron charge, and mass, respectively. Due to the population inversion in this model the oscillator strength is negative and its negative sign is included in Eq. (1) explicitly. In typical situations, the inequalities $\delta < \omega_p < \omega_0$ are obeyed. Based on these inequalities an arbitrary set of the parameters for the active Lorentzian medium is chosen as, $\omega_0 = 4.0 \times 10^{15}$ Hz, $\omega_p = 1.0 \times 10^{15}$ Hz, $\delta = 0.2 \times 10^{15}$ Hz. Figure 1 shows the plot of the real part of the refractive index of the medium in inverted state ($f < 0$) and in ground state ($f > 0$). The important assumptions are that the system responds linearly to the classical electromagnetic field theory and has a causal response, so that the Kramers-Kronig relations are valid. Based on Fig. 1 in the region below the resonance the index is less than 1 and one expects to observe negative or superluminal group velocity when the frequency distribution of a signal is located in this region.

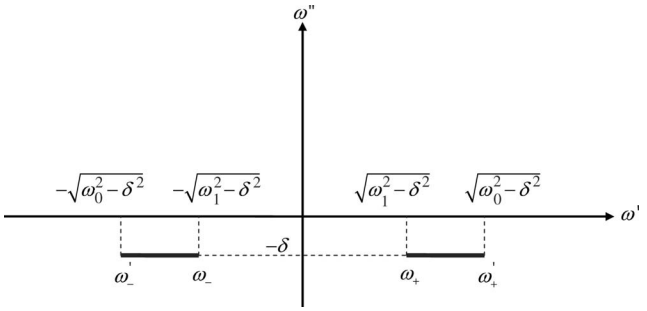

FIG. 2. Branch points and branch cuts for the active single resonance Lorentzian medium.

The branch points for $n(\omega)$, and hence, for $\phi(\omega)$, can be directly determined by rewriting the complex refractive index as

$$n(\omega) = \left(\frac{\omega^2 - \omega_1^2 + 2\delta i\omega}{\omega^2 - \omega_0^2 + 2\delta i\omega}\right)^{1/2} = \left(\frac{(\omega-\omega_+)(\omega-\omega_-)}{(\omega-\omega_+')(\omega-\omega_-')}\right)^{1/2}, \tag{3}$$

where

$$\omega_1^2 = \omega_0^2 - \omega_p^2. \tag{4}$$

The branch point locations are given by

$$\omega_\pm = \pm\sqrt{\omega_1^2 - \delta^2} - i\delta, \quad \omega_\pm' = \pm\sqrt{\omega_0^2 - \delta^2} - i\delta. \tag{5}$$

It is assumed that $\omega_0 > \delta$ and $\omega_1 > \delta$; therefore, both branch points lie along the line $\omega'' = -\delta$ symmetrically located about the imaginary axis. The branch lines chosen here consists of the line segments $\omega_-'\omega_-$ and $\omega_+\omega_+'$, as shown in Fig. 2. The complex refractive index $n(\omega)$ and the phase function $\phi(\omega)$ are analytic in the complex ω-plane, except at the branch points $\omega_\pm'$ and $\omega_\pm$.

III. SUPERLUMINAL PROPAGATION IN AN ACTIVE LORENTZIAN MEDIUM

As mentioned before, the possibility of superluminal propagation in an inverted two-level atomic medium was first considered by Chiao [10]. When the carrier frequency detuned far outside the resonance frequency, on the low frequency side the group velocity can be superluminal and for a sufficiently long medium the exit pulse is well resolved from a companion pulse traveling through an equal distance in free space. In this simulation, inverse Fourier transform method is used to calculate the time advancement of a Gaussian modulated signal propagating in an active Lorentzian media. The input modulated Gaussian pulse propagating in the positive z direction is given by

$$S(t) = \exp\left[-\left(\frac{t-t_0}{T_s}\right)^2\right]\sin(\omega_c t), \tag{6}$$

where ω_c is the carrier frequency and the pulse is centered around the time $t_0 > 0$ at the $z = 0$ plane with a full width at $1/e$ point given by $2T_s$. In this simulation the excitation pa-

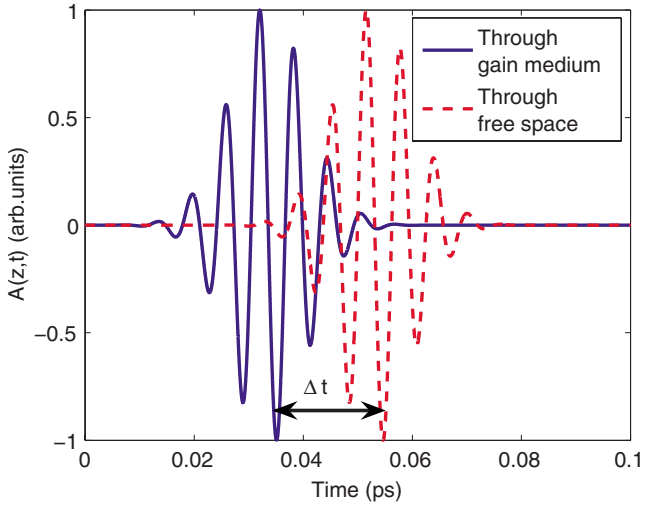

FIG. 3. (Color online) Pulse advancement in an active medium at $z=1$ μm ($\Delta t=0.0195$ ps).

rameters are $\omega_c=1\times10^{15}$ Hz, $T_s=1\times10^{-14}$ s, and $t_0=3.035\times10^{-14}$ s. Figure 3 shows the normalized electric field of the Gaussian pulse that has traveled the same length though the active medium and free space. The peak of the pulse that has traveled through the active medium reaches the sampling point at $z=1$ μm approximately 0.0195 ps sooner than the pulse that has traveled through the free space. The interesting question is whether or not the abnormal behavior observed in Fig. 3 is consistent with the requirements of special relativity, which demands no information to be transmitted faster than the speed of light in vacuum. An information carrying signal that is physically realizable is a causal signal that has a beginning in time and space ("front"). Consequently, in a noiseless channel (as we have considered in all the simulations), the earliest time that the future value of the information carrying signal can be predicted is $t=0^+$, since $t=0$ by definition is a point of nonanalyticity for which the Taylor expansion does not exist. Therefore, the genuine information regarding the correct value of a causal signal is contained within the time interval beginning with $t=0$ (the "front") and times immediately following it (precursors).

The excitation in Fig. 3 has a very smooth turn-on (the amplitude of the pulse at the turn-on point is approximately e^{-9}, whereas the peak amplitude is unity), therefore, the effects of the front are not easily observed at the output. To observe the evolution of the front, we have studied the evolution of a modulated step excitation that has a sharp turn on in the beginning, hence, the effect of the front can clearly be seen in the signal evolution. We have used the steepest descent method to calculate the propagation of the pulse inside the active medium. It gives us a complete description of the time evolution of the signal and its relation to the phase topography in the complex ω-plane.

IV. INTEGRAL DESCRIPTION OF THE PLANE WAVE PROPAGATION IN DISPERSIVE MEDIA

The integral representation of an arbitrary plane electromagnetic wave propagated in the positive z direction through a linear, homogeneous, isotropic, temporally dispersive medium occupying the half-space $z>0$ is given by [21]

$$A(z,t)=\frac{1}{2\pi}\int_C \tilde{f}(\omega)\exp\{i[\tilde{k}(\omega)z-\omega t]\}d\omega, \tag{7}$$

where the complex wave number $\tilde{k}(\omega)$ is given by

$$\tilde{k}(\omega)=\frac{\omega}{c}n(\omega), \tag{8}$$

with $n(\omega)$ being the complex index of refraction of the dispersive medium. Here, $\tilde{f}(\omega)$ is the Fourier transform of the initial pulse $f(t)=A(0,t)$ at the input plane at $z=0$ and $A(z,t)$ represents any scalar component of the electric field or magnetic field. In Eq. (7) for purposes of convergence, the contour of integration C in the complex ω-plane is the straight line $\omega=\omega'+ia$, where $\omega'=\mathrm{Re}(\omega)$ ranges from negative to positive infinity and a is a fixed positive constant that is greater than the abscissa of absolute convergence for the function $f(t)$ [33–35] (real and imaginary parts of a complex function are written as $\mathrm{Re}\{\cdots\}$ and $\mathrm{Im}\{\cdots\}$ in this paper). Another form of Eq. (7) which is suitable for asymptotic methods is

$$A(z,\theta)=\frac{1}{2\pi}\int_C \tilde{f}(\omega)\exp\left(\frac{z}{c}\phi(\omega,\theta)\right)d\omega, \tag{9}$$

where $\theta=ct/z$ is a dimensionless space-time parameter and

$$\phi(\omega,\theta)=i\omega[n(\omega)-\theta] \tag{10}$$

is a complex phase function. Based on the properties of the Lorentzian model as a physically permissible model and the fact that the excitation is real, the propagated field can be written as [21],

$$A(z,\theta)=\frac{1}{2\pi}\mathrm{Re}\left[\int_{-\infty+ia}^{+\infty+ia}\tilde{f}(\omega)\exp\left(\frac{z}{c}\phi(\omega,\theta)\right)d\omega\right]. \tag{11}$$

In the case of a modulated excitation with carrier frequency ω_c, namely,

$$f(t)=u(t)\sin(\omega_c t), \tag{12}$$

where $u(t)$ is a unit step signal given as

$$u(t)=\begin{cases}0 & \text{for } t<0,\\ 1 & \text{for } t>0,\end{cases} \tag{13}$$

the integral representation of the propagated field is

$$A(z,\theta)=-\frac{1}{2\pi}\mathrm{Re}\left[\int_{-\infty+ia}^{+\infty+ia}\frac{1}{\omega-\omega_c}\exp\left(\frac{z}{c}\phi(\omega,\theta)\right)d\omega\right], \tag{14}$$

for $t>0$ and is zero for $t<0$. The asymptotic calculation of the integral in Eq. (14) is presented in the next section.

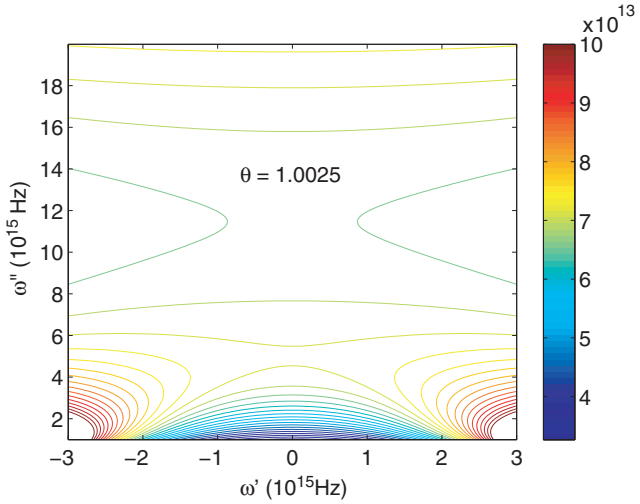

FIG. 4. (Color online) Contours of $X(\omega,\theta)$ on the upper-half of the complex ω-plane for $\theta=1.0025$.

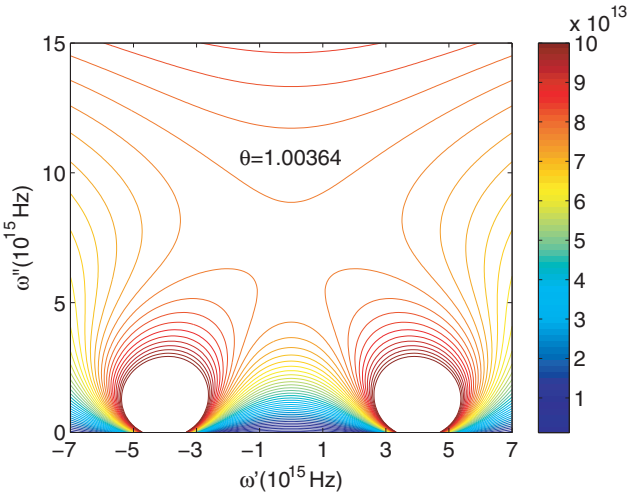

FIG. 5. (Color online) Contours of $X(\omega,\theta)$ on the upper-half of the complex ω-plane for $\theta=1.003\,64$.

V. ASYMPTOTIC ANALYSIS OF THE PROPAGATION OF A MODULATED STEP PULSE IN AN ACTIVE LORENTZIAN MEDIUM

Asymptotic analysis of the integral in Eq. (14) includes three steps. The first step is to determine the topography of $X(\omega,\theta)$, the real part of the complex phase function $[\phi(\omega,\theta)=X(\omega,\theta)+iY(\omega,\theta)]$, on the complex ω-plane. The second step is to determine the location of the saddle points of $\phi(\omega,\theta)$. With all the information in hand, the third step is to calculate the total field at each value of θ for a predefined observation point.

A. Numerical calculation of the topography of $X(\omega,\theta)$

In this section we will study the behavior of $X(\omega,\theta)=\mathrm{Re}\{\phi(\omega,\theta)\}$ with contour plots of $X(\omega,\theta)$ in the upper half of the complex ω-plane. These plots give us a picture of the topography of $X(\omega,\theta)$ in order to determine the number of saddle points of $\phi(\omega,\theta)$ and their locations. These plots can also be used to find the approximate locations of the deformed contour of integration that passes through these saddle points. Using medium parameters $\omega_0=4.0\times10^{15}$ Hz, $\omega_p=1.0\times10^{15}$ Hz, $\delta=0.2\times10^{15}$ Hz the contours of the real phase function $X(\omega,\theta)$ in the upper half of the complex ω-plane are plotted in Figs. 4–6 for different values of the parameter θ. In Fig. 4 the value of θ is very close to 1 and we can clearly see two first order saddle points on the imaginary axis. Comparing the value of $X(\omega,\theta)$ at the location of the saddle points shows that the saddle point that is closer to the origin is dominant. In Fig. 5, at $\theta=1.003\,64$, the two saddle points coalesce into one second order saddle point. In Fig. 6, θ is greater than $\theta=1.0036$ and the two first order saddle points appear symmetrically on both sides of the imaginary axis.

B. Numerical determination of the location of the saddle points

In this section we numerically calculate the exact locations of the saddle points in the complex ω-plane. The phase function $\phi(\omega,\theta)$ is stationary at a saddle point, therefore,

$$\phi'(\omega,\theta)=i[n(\omega)-\theta]+i\omega n'(\omega)=0, \tag{15}$$

where prime represents the first order derivative with respect to ω. Using the expression for the complex refractive index, [Eq. (1)] the saddle point locations are given by the solution of the equation

$$\left(1+\frac{\omega_p^2}{\omega^2-\omega_0^2+2\delta i\omega}\right)^{1/2} - \frac{\omega_p^2\omega(\omega+\delta i)}{\omega^2-\omega_0^2+2\delta i\omega\left[\left(1+\frac{\omega_p^2}{\omega^2-\omega_0^2+2\delta i\omega}\right)^{1/2}\right]} - \theta = 0. \tag{16}$$

Based on the phase plots in Figs. 4–6 we can picture the path of the saddle points in the complex ω-plane. Figure 7 shows a general picture of the two saddle points path that are

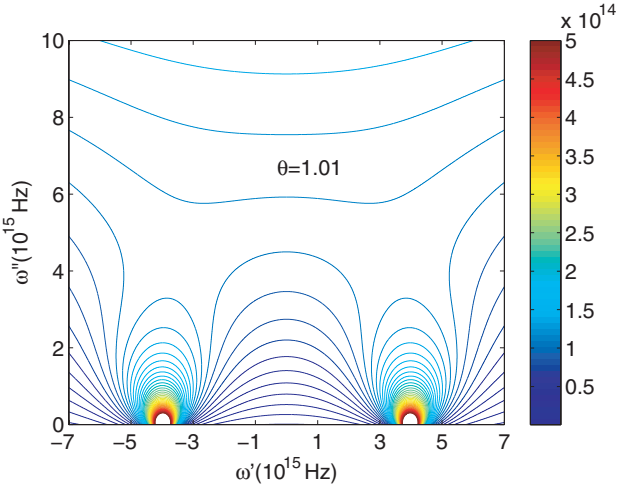

FIG. 6. (Color online) Contours of $X(\omega,\theta)$ on the upper-half of the complex ω-plane for $\theta=1.01$.

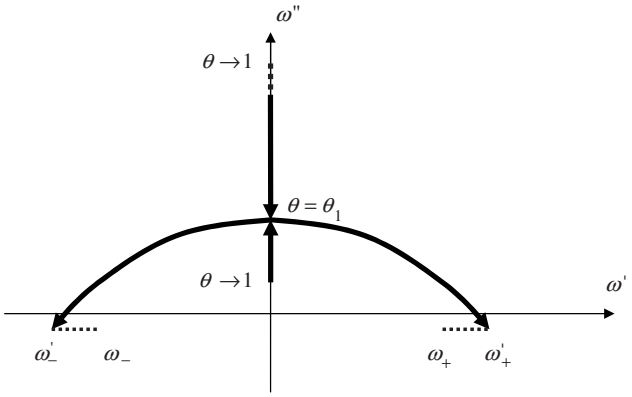

FIG. 7. Locations of the upper-half-plane saddle points as a function of θ.

above the branch cuts in the complex ω-plane. The other two saddle points evolve in a similar manner that is symmetric with respect to the branch cuts. After some manipulation, Eq. (16) turns into an eight order polynomial. The phase plots help us to identify the four roots that are the saddle points of the phase function on the complex ω-plane. The numerical results for the saddle points locations as a function of θ are plotted in Fig. 8. The saddle points in the upper-half-plane (SP_{UHP}) are on the imaginary axis for $\theta=1$ and as θ increases from unity one of them moves down from infinity on the imaginary ω axis and the other one moves up on the imaginary axis [Fig. 8(a)]. At $\theta=\theta_1=1.003\,64$ these two saddle points join together and form a second order saddle point. For θ greater than θ_1 two first order saddle points leave the imaginary axis symmetrically, in opposite directions and move towards the branch points [Fig. 8(b)]. As $\theta\to+\infty$ the UHP saddle points get very close to the branch points ω'_+ and ω'_-. The saddle points on the lower-half-plane (SP_{LHP}) are on the imaginary axis at $\theta=1$ and as θ increases from unity one

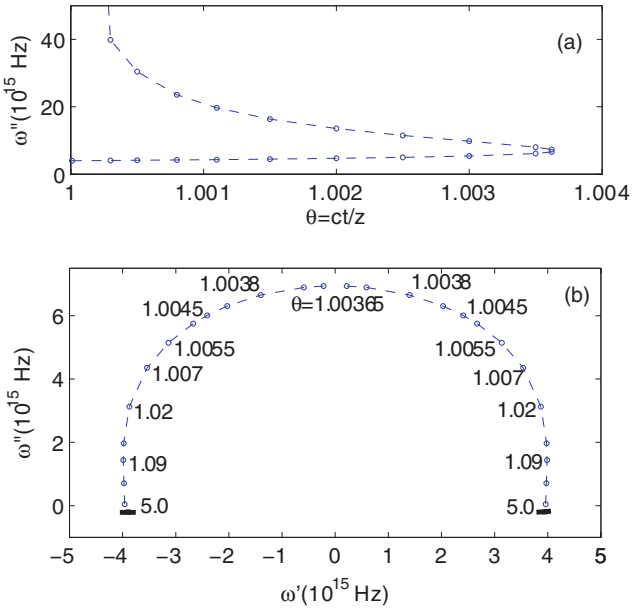

FIG. 8. (Color online) Locations of the upper-half-plane saddle points as a function of θ (a) $1<\theta<\theta_1$, (b) $\theta>\theta_1$.

of them moves down and the other one moves up and at $\theta=1.0043$ they join together and form a second order saddle point. As θ increases they leave the imaginary axis and move towards the branch points symmetric with respect to the imaginary axis in opposite directions.

C. Asymptotic calculation of the field $A(z,\theta)$

Equipped with the knowledge of the topography of the phase function $\phi(\omega,\theta)$ and the dynamics of its saddle points, it is now possible to perform the asymptotic calculation of the field $A(z,\theta)$ as given by Eq. (14). The first step in the asymptotic calculation of the field $A(z,\theta)$ is to deform the original contour of integration to the steepest descent path. It is assumed that $\tilde{u}(\omega-\omega_c)$ (the Fourier transform of the modulated unit step excitation) is analytic in the complex ω-plane except for a countable number of isolated points where it may have poles. For our modulated unit step function, $u(t)$, the Fourier transform, $\tilde{u}(\omega-\omega_c)$ only has a single pole at $\omega=\omega_c=1\times10^{15}$ Hz. The contribution of the simple pole singularity at $\omega=\omega_c$ occurs when the original integration path passes the pole at ω_c. We assume that the original path of integration and the steepest descent path lie on the same side of the pole for $\theta<\theta_s$ and on opposite sides for $\theta>\theta_s$ (at $\theta=\theta_s$ the real part of the phase function at the saddle point that interacts with the pole is equal to the real part of the phase function at the frequency of the pole).

The asymptotic approximation of the field $A(z,\theta)$ is [36,21]

$$A(z,\theta)=A_{sp}(z,\theta)+A_c(z,\theta), \tag{17}$$

where, A_{sp} is the contribution of the saddle points and A_c is the contribution of the pole. As mentioned before for values of θ close to 1 there are two saddle points in the UHP of the complex ω-plane. The one that moves upwards is the dominant saddle point, therefore, for $1<\theta<\theta_1$, the contribution of the saddle points is given as

$$A_{sp}(z,\theta)\sim \mathrm{Re}\left(\sqrt{\frac{-2\pi}{(z/c)\phi''(\omega_{sp},\theta)}}\tilde{f}(\omega_{sp})e^{(z/c)\phi(\omega_{sp},\theta)}\right),$$

$$z\to\infty, \tag{18}$$

where $\phi''(\omega_c,\theta)$ is the second derivative of the $\phi(\omega,\theta)$ with respect to frequency at $\omega=\omega_c$. At $\theta=\theta_1$ the two saddle points on the upper-half of the imaginary axis join and form a second order saddle point. The contribution of the saddle points at θ_1 is given as

$$A_{sp}(z,\theta_1)\sim \mathrm{Re}\left[e^{(z/c)\phi(\omega_{sp},\theta)}\Gamma\left(\frac{1}{3}\right)[a_0^+(\omega_{sp},\theta)-a_0^-(\omega_{sp},\theta)]\times\left(\frac{c}{z}\right)^{1/3}\right],\quad z\to\infty, \tag{19}$$

where $\Gamma(\cdots)$ is the well-known gamma function and

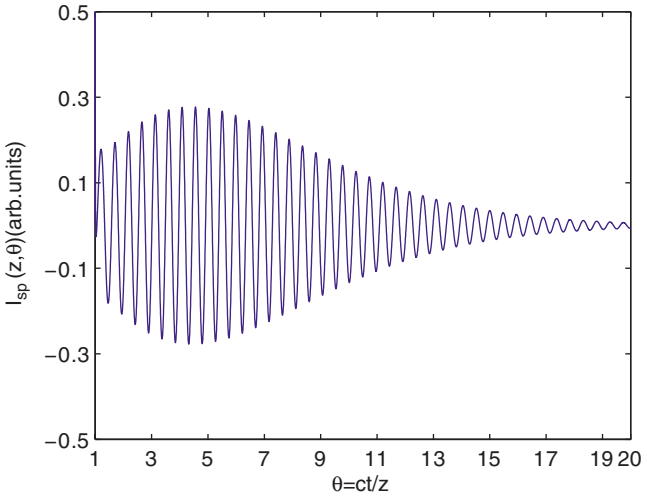

FIG. 9. (Color online) The part of the total sampled field 1 μm inside the active medium due to the saddle points.

$$a_0(\omega_{sp},\theta) = \frac{\tilde{f}(\omega_{sp})}{3}\left(\frac{-\phi^{(3)}(\omega_{sp},\theta)}{3!}\right)^{(-1/3)}. \tag{20}$$

The terms a_0^+ and a_0^- are different values of the multivalue complex function, a_0, for the integration paths which extend from ω_{sp} to $+\infty$ and from ω_{sp} to $-\infty$, respectively. The term $\phi^{(3)}(w)$ which is the third derivative of $\phi(\omega)$ with respect to frequency.

As θ increases ($\theta > \theta_1$) the saddle points on the UHP leave the imaginary axis and move away from the imaginary axis in opposite directions. One of these saddle points moves towards the branch cut on the right-half-plane and the other one moves towards the branch cut on the left-half-plane. Therefore, the integration path for $\theta > \theta_1$ goes through two first order saddle points and the contribution of these saddle points is given as

$$A_{sp}(\omega,\theta) = A_{sp}^r(\omega,\theta) + A_{sp}^l(\omega,\theta), \tag{21}$$

where $A_{sp}^r(\omega,\theta)$ and $A_{sp}^l(\omega,\theta)$ are the contributions of the first order saddle points on the right- and left-half-planes, respectively. Both $A_{sp}^r(\omega,\theta)$ and $A_{sp}^l(\omega,\theta)$ are calculated using Eq. (18). Figure 9 shows the portion of the pulse that is due to the saddle points.

The residue contribution of the pole appears for $\theta > \theta_s$, where, the value of θ_s is given by the expression

$$X(\omega_{sp},\theta_s) = X(\omega_c,\theta_s), \tag{22}$$

where ω_{sp} is the saddle point that interacts with the pole singularity. The terms $X(\omega_{sp},\theta)$ and $X(\omega_c,\theta)$ are the real part of the phase function at the angular frequency of the corresponding saddle point and the pole of the excitation at each value of θ, respectively. The contribution of the pole, $A_c(z,\theta)$ is given as

$$A_c(z,\theta) = -2\pi i\,\mathrm{Re}[\Lambda(\theta)], \tag{23}$$

where

$$\Lambda(\theta) = 0 \quad \text{for } \theta < \theta_s, \tag{24}$$

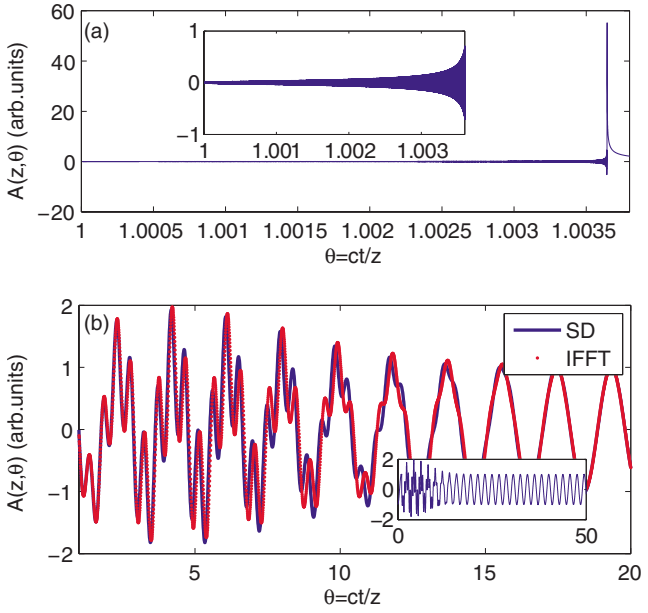

FIG. 10. (Color online) Total sampled field at 1 μm inside the active medium for (a) $1 < \theta < 1.0038$; (b) $1.0038 < \theta < 25$ calculated using the steepest descent (SD) and inverse fast Fourier transform (IFFT) methods ($\delta = 0.1 \times 10^{15}$, $\omega_0 = 4.0 \times 10^{15}$ Hz, $\omega_p = 1.0 \times 10^{15}$ Hz, $\omega_c = 1 \times 10^{15}$ Hz).

$$\Lambda(\theta_s) = \frac{1}{2}\frac{1}{2\pi} i\gamma e^{(z/c)\phi(\omega_c,\theta_s)} \quad \text{for } \theta = \theta_s, \tag{25}$$

$$\Lambda(\theta) = \frac{1}{2\pi} i\gamma e^{(z/c)\phi(\omega_c,\theta)} \quad \text{for } \theta > \theta_s, \tag{26}$$

where

$$\gamma = \lim_{\omega\to\omega_c}[(\omega-\omega_c)\tilde{f}(\omega)]. \tag{27}$$

The asymptotic approximation of the total field 1 μm inside the active Lorentzian is plotted in Fig. 10(a) for $1 < \theta < 1.0038$ and Fig. 10(b) for $1.0038 < \theta < 14$. As it can be seen from the inset of Fig. 10(a) there is high frequency oscillation for $1 < \theta < \theta_1$ that is due the saddle points on the imaginary axis. At $\theta = \theta_s = 1.23$ the steepest descent path passes the pole and the transient, due to both the saddle points and the pole that appear. As θ increases the contribution of the saddle points fades and the steady-state part of the signal that is solely due to the pole becomes dominant. The result presented here is validated using the inverse Fourier transform technique [37] for $1.0038 < \theta < 14$ in Fig. 10(b). There is good agreement between the two techniques. The number of points needed to confirm the asymptotic result in the range $1 < \theta < 1.0038$ is extremely large and cannot be practically calculated via the Fourier transform. It shows that asymptotic techniques such as steepest descent method are powerful in studying the transient response in dispersive media.

As demonstrated in Sec. III, the peak of a Gaussian pulse can travel with a superluminal group velocity inside an ac-

tive Lorentzian medium. Considering the case of a step-like envelope excitation that is zero for $t<0$, the following observation can be made. At $z=0$, the propagated field inside the medium can be nonzero for $\theta<1$ only if the field propagates with a front velocity greater than the vacuum speed of light c which violates the principle of relativistic causality. The asymptotic calculations provide the description of the temporal evolution of the signal for $t\geqslant 0$. However, it can be mathematically proved that no signal (information) may be detected before $t=0$, by the contour integration of Eq. (11). First, the integral of Eq. (11) can be evaluated by closing the contour over the upper-half-plane. Moreover, the requirement that the medium is causal and that the incident signal has a "front," can be employed to show that the value of the integral is identically zero for $\theta<1$ (for velocities that are less than the speed of light, c). The detailed mathematical proof, which is based on Jordan's lemma and the Cauchy theorem, can be found in [22].

VI. COMPARISON OF THE PASSIVE AND ACTIVE LORENTZIAN

As mentioned in Sec. II, the complex index of refraction of the active Lorentzian, ignoring the effect of inhomogeneous line broadening, is similar to the passive Lorentzian index, except for the sign of the oscillator strength which is negative. For both active and passive media, the index of refraction and therefore, the phase function, have two poles and two zeros on the complex ω-plane. Hence, in both cases the phase function has four saddle points. On the other hand, the evolution of the saddle points in these two media is completely different. In passive Lorentzian, the pair of the saddle points which corresponds to the Sommerfeld precursors is at $|\omega|\rightarrow\infty$ for $\theta\rightarrow 1$, while the pair of the saddle points which corresponds to the Brillouin precursors is on the imaginary axis. Both sets move towards the branch points as θ increases. For the active medium, all four saddle points are on the imaginary axis as $\theta\rightarrow 1$. As mentioned in Sec. V B, a pair of saddle points is on the positive imaginary axis and a second pair is on the negative imaginary axis. Moreover, in the passive medium case, the saddle points at $|\omega'|\rightarrow\infty$ are dominant for $\theta\rightarrow 1$. As θ increases (yet before the excitation pole becomes dominant), the second pair of saddle points, which are close to origin, tends to dominate. In the active medium case, the saddle point which moves upwards on the positive imaginary axis is dominant for $\theta\rightarrow 1$ and as θ increases the excitation pole becomes dominant. The physical meaning of these differences in the evolution of the saddle points is as follows. While both Sommerfeld and Brillouin precursors can be excited in passive media, the former are not present in active media. In addition, the transient part of the signal (which is due to the saddle points) and the main part of the signal (which is due the pole of the excitation) appear almost concurrently. (See Refs. [38–41].)

VII. SUMMARY AND DISCUSSION

This paper presented a study of pulse propagation in an active Lorentzian media, aimed at illuminating their transient response. It was shown that while superluminal group velocities are possible in such media, these velocities are compatible with relativistic causality. In particular, the causal propagation of the front of a Gaussian pulse inside an active medium was demonstrated, despite the fact that the pulse envelope itself was propagating superluminally. Then, the steepest descent method was employed for the thorough investigation of the transient response of active media, with the goal of identifying precursor fields that can be supported in these media, along the lines of the passive case. In particular, the propagation of a step-modulated signal was studied. It was shown that Sommerfeld precursors are not excited in active media, while the transient part of a propagating signal is almost indistinguishable from the main part. These observations are in stark contrast with the evolution of distinct Sommerfeld and Brillouin precursor fields prior to the main signal in passive Lorentzian media. More accurate description of the signal evolution in active media can be achieved using a higher order approximation for the propagation integral. Note that our study does not include saturation and associated nonlinear effects in active media. The study of their impact on the transient response of the medium can be the subject of future work.

ACKNOWLEDGMENTS

This work was supported by the Natural Sciences and Engineering Research Council of Canada under Grant No. 249531-02, and in part by Photonic Research Ontario, Contract No. 72022792.

[1] A. Ranfagni, D. Mugnai, P. Fabeni, and G. P. Pazzi, Appl. Phys. Lett. **58**, 774 (1991).
[2] A. Ranfagni and D. Mugnai, Phys. Rev. E **54**, 5692 (1996).
[3] D. Mugnai, A. Ranfagni, and L. Ronchi, Phys. Lett. A **247**, 281 (1998).
[4] M. Mojahedi, E. Schamiloglu, F. Hegeler, and K. J. Malloy, Phys. Rev. E **62**, 5758 (2000).
[5] M. Mojahedi, E. Schamiloglu, K. Agi, and K. J. Malloy, IEEE J. Quantum Electron. **36**, 418 (2000).
[6] A. Enders and G. Nimtz, Phys. Rev. B **47**, 9605 (1993).
[7] C. Spielmann, R. Szipocs, A. Stingl, and F. Krausz, Phys. Rev. Lett. **73**, 2308 (1994).
[8] A. M. Steinberg, P. G. Kwiat, and R. Y. Chiao, Phys. Rev. Lett. **71**, 708 (1993).
[9] A. M. Steinberg and R. Y. Chiao, Phys. Rev. A **51**, 3525 (1995).
[10] R. Y. Chiao, Phys. Rev. A **48**, R34 (1993).
[11] E. L. Bolda, R. Y. Chiao, and J. C. Garrison, Phys. Rev. A **48**, 3890 (1993).
[12] E. L. Bolda, J. C. Garrison, and R. Y. Chiao, Phys. Rev. A **49**,

2938 (1994).
[13] R. Y. Chiao and J. Boyce, Phys. Rev. Lett. **73**, 3383 (1994).
[14] L. J. Wang, A. Dogariu, and A. Kuzmich, Nature (London) **406**, 277 (2001).
[15] M. D. Stenner, D. J. Gauthier, and M. A. Neifeld, Nature (London) **425**, 695 (2003).
[16] J. F. Woodley and M. Mojahedi, Phys. Rev. E **70**, 046603 (2004).
[17] R. Safian, C. D. Sarris, and M. Mojahedi, Phys. Rev. E **73**, 066602 (2006).
[18] O. F. Siddiqui, S. J. Erickson, G. V. Eleftheriades, and M. Mojahedi, IEEE Trans. Microwave Theory Tech. **52**, 1449 (2004).
[19] S. J. Erickson, M. Khaja, and M. Mojahedi, AP-S International Symposium and USNC/URSI National Radio Science Meeting, Washington, D.C., 2005.
[20] L. Brillouin, *Wave Propagation and Group Velocity* (Academic, New York, 1960).
[21] K. E. Oughstun and G. C. Sherman, *Electromagnetic Pulse Propagation in Causal Dielectrics* (Springer-Verlag, Berlin, 1994).
[22] K. E. Oughstun and G. C. Sherman, J. Opt. Soc. Am. B **5**, 817 (1988).
[23] K. E. Oughstun, J. Opt. Soc. Am. A **6**, 1394 (1989).
[24] K. E. Oughstun and G. C. Sherman, Phys. Rev. A **41**, 6090 (1990).
[25] C. M. Balictsis and K. E. Oughstun, Phys. Rev. E **47**, 3645 (1993).
[26] C. M. Balictsis and K. E. Oughstun, Phys. Rev. E **55**, 1910 (1997).
[27] H. Xiao and K. E. Oughstun, J. Opt. Soc. Am. B **16**, 1773 (1999).
[28] H. L. Bertoni, L. Carin, and L. B. Felsen, *Ultra-Wideband, Short-Pulse Electromagnetics* (Plenum, New York, 1993).
[29] L. Carin and L. B. Felsen, *Ultra-Wideband, Short-Pulse Electromagnetics* (Plenum, New York, 1995), Vol. 2.
[30] C. E. Baum, L. Carin, and A. P. Stone, *Ultra-Wideband, Short-Pulse Electromagnetics* (Plenum, New York, 1997), Vol. 3.
[31] E. Heyman, B. Melbaum, and J. Shiloh, *Ultra-Wideband, Short-Pulse Electromagnetics* (Plenum, New York, 1999), Vol. 4.
[32] P. D. Smith and S. R. Cloude, *Ultra-Wideband, Short-Pulse Electromagnetics* (Plenum, New York, 2002), Vol. 5.
[33] J. A. Stratton, *Electromagnetic Theory* (McGraw-Hill, New York, 1941).
[34] E. T. Copson, *An Introduction to the Theory of Functions of a Complex Variable* (Oxford University Press, London, 1972).
[35] M. J. Ablowitz and A. S. Fokas, *Complex Variables: Introduction and Application*, 2nd ed. (Cambridge University Press, Cambridge, 1977).
[36] L. B. Felsen and N. Marcuvitz, *Radiation and Scattering of Waves* (Prentice-Hall, Englewood Cliffs, NJ, 1973).
[37] L. Borgman and S. J. Erickson, Comput. Geosci. **7**, 99 (1981).
[38] R. Y. Chiao and A. M. Steinberg, Prog. Opt. **37**, 345 (1997).
[39] S. Chu and S. Wong, Phys. Rev. Lett. **49**, 1293 (1982).
[40] M. W. Mitchell and R. Y. Chiao, Phys. Lett. A **230**, 133 (1997).
[41] R. Y. Chiao, A. E. Kozhekin, and G. Kurizki, Phys. Rev. Lett. **77**, 1254 (1996).